Photochemistry and Photobiology, 2002, 75(6): 652–661

The Peripheral Benzodiazepine Receptor in Photodynamic Therapy with the Phthalocyanine Photosensitizer Pc 4¶

Rachel L. Morris[1], Marie E. Varnes[1,2], Malcolm E. Kenney[2,3], Ying-Syi Li[3], Kashif Azizuddin[1], Maureen W. McEnery[4] and Nancy L. Oleinick*[1,2]

[1]Department of Radiation Oncology,
[2]The CWRU/Ireland Comprehensive Cancer Center and Departments of
[3]Chemistry and [4]Physiology and Biophysics, Case Western Reserve University, Cleveland, OH

Received 5 November 2001; accepted 1 March 2002

ABSTRACT

The peripheral benzodiazepine receptor (PBR) is an 18 kDa protein of the outer mitochondrial membrane that interacts with the voltage-dependent anion channel and may participate in formation of the permeability transition pore. The physiological role of PBR is reflected in the high-affinity binding of endogenous ligands that are metabolites of both cholesterol and heme. Certain porphyrin precursors of heme can be photosensitizers for photodynamic therapy (PDT), which depends on visible light activation of porphyrin-related macrocycles. Because the apparent binding affinity of a series of porphyrin analogs for PBR paralleled their ability to photoinactivate cells, PBR has been proposed as the molecular target for porphyrin-derived photocytotoxicity. The phthalocyanine (Pc) photosensitizer Pc 4 accumulates in mitochondria and structurally resembles porphyrins. Therefore, we tested the relevance of PBR binding on Pc 4–PDT. Binding affinity was measured by competition with ^{3}H-PK11195, a high-affinity ligand of PBR, for binding to rat kidney mitochondria (RKM) or intact Chinese hamster ovary (CHO) cells. To assess the binding of the Pc directly, we synthesized ^{14}C-labeled Pc 4 and found that whereas Pc 4 was a competitive inhibitor of ^{3}H-PK11195 binding to the PBR, PK11195 did not inhibit the binding of ^{14}C–Pc 4 to RKM. Further, ^{14}C–Pc 4 binding to RKM showed no evidence of saturation up to 10 μ*M*. Finally, when Pc 4–loaded CHO cells were exposed to activating red light, apoptosis was induced; Pc 4–PDT was less effective in causing apoptosis in a companion cell line overexpressing the antiapoptotic protein Bcl-2. For both cell lines, PK11195 inhibited PDT-induced apoptosis; however, the inhibition was transient and did not extend to overall cell death, as determined by clonogenic assay. The results demonstrate (1) the presence of low-affinity binding sites for Pc 4 on PBR; (2) the presence of multiple binding sites for Pc 4 in RKM and CHO cells other than those that influence PK11195 binding; and (3) the ability of high supersaturating levels of PK11195 to transiently inhibit apoptosis initiated by Pc 4–PDT, with less influence on overall cell killing. We conclude that the binding of Pc 4 to PBR is less relevant to the photocytotoxicity of Pc 4–PDT than are other mitochondrial events, such as photodamage to Bcl-2 and that the observed inhibition of Pc 4–PDT–induced apoptosis by PK11195 likely occurs through a mechanism independent of PBR.

INTRODUCTION

Photodynamic therapy (PDT), an innovative approach to the treatment of cancer and noncancerous conditions, utilizes a photosensitive compound that is activated by visible light. To date, PDT has been used to treat thousands of patients worldwide, and it has been approved by the US FDA for lung and esophageal cancer, actinic keratoses and age-related macular degeneration (1).

Most photosensitizers under investigation for PDT are porphyrin-related macrocycles that are lipophilic and efficient generators of singlet oxygen (2). In general, PDT mechanisms are thought to be initiated when a photoexcited membrane-localized photosensitizer transfers energy of the excited triplet state to molecular oxygen to generate singlet oxygen (1). Subsequent oxidation–reduction reactions can also produce superoxide anions, hydrogen peroxide and hydroxyl radicals. The short half-life of reactive oxygen species (ROS), especially singlet oxygen and hydroxyl radical, dictates that they react with cellular components that are within a few nanometers of their formation sites in membranes. Establishing the binding site for a photosensitizer

¶Posted on the website on 27 March 2002.

*To whom correspondence should be addressed at: Department of Radiation Oncology, School of Medicine (BRB-324), Case Western Reserve University, 10900 Euclid Avenue, Cleveland, OH 44106-4942, USA. Fax: 216-368-1142; e-mail: nlo@po.cwru.edu

Abbreviations: BSA, bovine serum albumin; CHO, Chinese hamster ovary; DMF, dimethylformamide; MSH, 220 m*M* mannitol, 70 m*M* sucrose, 2 m*M* *N*-2-hydroxyethyl-piperazine *N*′-2-ethanesulfonic acid, 1 mg/mL BSA, pH 7.4; NMR, nuclear magnetic resonance; PBR, peripheral benzodiazepine receptor; PBS, phosphate-buffered saline; Pc, phthalocyanine; PDT, photodynamic therapy; PPIX, protoporphyrin IX; PTPC, permeability transition pore complex; RKM, rat kidney mitochondria; ROS, reactive oxygen species; TB, 50 m*M* Tris (pH 7.7) + 0.1% BSA; VDAC, voltage-dependent anion channel.

then can allow potential molecular targets of ROS photochemistry to be approached.

Several photosensitizers bind somewhat preferentially to mitochondria, and damage to the mitochondria occurs early upon photoirradiation (3,4). In many cases, cells die by apoptosis (5–7). An early step in the pathway is the loss of the mitochondrial transmembrane potential and the release of proapoptotic mitochondrial factors, including cytochrome *c*, from the intermembrane space. In the cytosol, cytochrome *c* complexes with Apaf-1 and procaspase-9 to form the so-called ''apoptosome,'' which initiates caspase activation and the systematic cleavage of specific proteins and DNA that are characteristic of apoptosis (8,9).

One current model suggests that the loss of mitochondrial transmembrane potential and the release of proapoptotic mitochondrial factors result from the opening of a large conductance channel known as the permeability transition pore complex (PTPC) located at contact sites of the outer and inner mitochondrial membranes. The PTPC is thought to be a multimeric complex comprising several transmembrane proteins: (1) a 30 kDa inner membrane adenine nucleotide translocator; (2) a 32 kDa outer membrane voltage-dependent anion channel (VDAC) or mitochondrial porin; and (3) an 18 kDa outer membrane peripheral benzodiazepine receptor (PBR). In addition, members of the Bax–Bcl-2 family, cyclophilin D and enzymes of energy metabolism, such as hexokinase and mitochondrial creatine kinase, are also associated with components of the PTPC (10,11).

Because PTPC has not been reconstituted, its function in biological membranes is yet to be determined. Nevertheless, cross talk between components of PTPC has been demonstrated. For example, ligand binding to PBR induces changes in the conductance state of VDAC (12,13). In addition, evidence supports a role for PBR in the regulation of mitochondrial ion channel activity (14) and adenosine exchange between the mitochondria and cytoplasm (15).

Endogenous ligands of PBR include the diazepam-binding inhibitor and metabolites of cholesterol and heme that require mitochondrial import or export (16–20). An extensive series of reports by Verma, Snyder and coworkers (21–25) established porphyrins as endogenous ligands for PBR. Most prominent are dicarboxylic porphyrins, such as protoporphyrin IX (PPIX), that bind to PBR with nanomolar affinity. These authors also reported that a porphyrin's binding affinity to PBR correlated well with the ability of that porphyrin to photoinactivate cells, arguing that the PBR is an important subcellular target of PDT (26). That notion has recently been challenged, at least for certain positional isomers of PPIX, which showed differential binding affinity for PBR but identical ability to produce photodynamic cell death (27). A second challenge derives from a study demonstrating a correlation between PBR binding of porphyrins and hydrophobicity, the latter property correlating with PDT efficacy, within certain limits (28).

The silicon phthalocyanine (Pc) photosensitizer, Pc 4, is composed of the Pc macrocycle with a siloxypropyldimethylamine axial ligand on the central silicon. The Pc ring system is similar to the porphyrin ring system but is larger and contains significant structural differences. Furthermore, Pc are not found in nature and might therefore not normally interact with porphyrin-binding sites. Previous reports have established Pc 4–PDT as an efficient inducer of apoptosis (29,30). Recently, confocal microscopy studies have shown that the preferred sites of binding of Pc 4 are in the cytoplasmic membranes, in particular the mitochondria (31,32). Furthermore, Pc 4–PDT produces extensive photodamage to the antiapoptotic protein Bcl-2 (33), which is located on the mitochondrial outer membrane as well as on the nuclear membrane and the endoplasmic reticulum. Because the precise relationship between Bcl-2 photodamage and the induction of apoptosis by Pc 4–PDT remains unclear, it is appropriate to interrogate other possible mitochondrial targets, which might act in concert with photodamaged Bcl-2 or independently. The aim of the present study was to investigate the potential binding of Pc 4 to PBR. With the aid of the selective isoquinoline carboxamide ligand of PBR, PK11195, we find that Pc 4 can compete with PK11195 for binding to PBR of both isolated rat kidney mitochondria (RKM) and Chinese hamster ovary (CHO) cells but that much Pc 4 is bound to other sites as well. In addition, we demonstrate a transient PK11195 inhibition of Pc 4–PDT–mediated apoptosis.

MATERIALS AND METHODS

Materials

Pc 4 and ^{14}C–Pc 4 were dissolved in dimethylformamide (DMF) to provide stock solutions of 0.5 m*M* (34) and further diluted in ethanol. The stock solutions were stored in the dark at 4°C and were stable for at least 1 month after preparation. PPIX was purchased from Porphyrin Products (Logan, UT) and was dissolved in 1 *M* Tris to ~1 m*M* to provide a stock solution and then further diluted in 50 m*M* Tris (pH 7.7) + 0.1% bovine serum albumin (BSA) (TB). Pc 4 and PPIX stock concentrations were verified by absorption spectroscopy. ^{3}H-PK11195 (86 Ci/mmol) was purchased as an ethanol solution from NEN Life Science Products, Inc. (Boston, MA), and unlabeled PK11195 was purchased from Sigma Chemical Co. (St. Louis, MO). Radiolabeled and unlabeled PK11195 were dissolved and diluted in ethanol to produce stock solutions of 40 000 dpm/μL and 10 m*M*, respectively, and then further diluted in TB.

Preparation of RKM

Kidney mitochondria were isolated from male Sprague–Dawley rats. The rats were sacrificed by decapitation, kidneys were excised and immediately placed in ice-cold 220 m*M* mannitol, 70 m*M* sucrose, 2 m*M* *N*-2-hydroxyethyl-piperazine *N*′-2-ethanesulfonic acid, 1 mg/mL BSA, pH 7.4 (MSH). The tissue was rinsed, blotted, weighed and minced on ice. Then ice-cold MSH (10 mL/g wet wt) was added, and the tissue was homogenized using a Potter–Elvehjem homogenizer with three strokes of a loose-fitting pestle. The homogenate was centrifuged at 350 ***g*** for 10 min and the supernate saved. The pellet was dispersed in MSH and centrifuged again. The supernates were combined, and mitochondria were pelleted by centrifugation at 7000 ***g*** for 10 min. The pellet was washed two times and resuspended in MSH (0.2 mL/g wet wt). Protein concentration was determined using the Lowry assay, with BSA as standard (35). Some samples were centrifuged through a continuous 1.0–2.0 *M* sucrose gradient to increase purification (36). Mitochondria recovered from sucrose gradients did not differ significantly in respect to PBR ligand-binding properties from those prepared without that step. Data reported here reflect both protocols. Mitochondria were stored in 20 μL aliquots at ~50 mg/mL at −85°C.

Synthesis of $HOSiPcOSi(CH_3)_2(CH_2)_3N(CH_3)(^{14}CH_3)$, ^{14}C–Pc 4

$CH_3OSi(CH_3)_2(CH_2)_2I$, 1. A mixture of 3-chloropropyldimethylmethoxysilane (10.6 g, 70.0 mmol), NaI (20.8 g, 105 mmol) and acetone (100 mL) was refluxed for 2 days and filtered. The solid was washed with acetone, and the washings and filtrate were combined and concentrated to an oil by rotary evaporation (30°C). The oil was mixed with

ether (50 mL), and the resulting suspension was filtered. The solid was washed (ether), and the washings and the filtrate were combined and concentrated to an oil by rotary evaporation (30°C), and the oil was weighed (14.9 g, 82%). Nuclear magnetic resonance (NMR) (200 MHz, $CDCl_3$): δ 3.40 (s, 3H, CH_3O), 3.17 (m, 2H, $SiCH_2CH_2CH_2$), 1.84 (m, 2H, $SiCH_2CH_2CH_2$), 0.67 (m, 2H, $SiCH_2CH_2CH_2$), 0.08 (s, 6H, $SiCH_3$).

The compound is a yellow, mobile liquid. It is soluble in toluene, CH_2Cl_2 and DMF.

$SiPc[OSi(CH_3)_2(CH_2)_3I]_2$, ***Pc 59***. A mixture of iodopropylsilane **1** (1.80 g, 6.97 mmol), $SiPc(OH)_2$ (401 mg, 0.698 mmol) and xylene (300 mL) was slowly distilled for 6 h (~35 mL of distillate) and then concentrated to a slurry by rotary evaporation (50°C). The slurry was diluted with an ethanol–H_2O solution (1:1, 50 mL) and filtered, and the solid was washed (ethanol; 1:1 ethanol–H_2O solution), vacuum dried (60°C) and weighed (567 mg, 77% based on $SiPc(OH)_2$). Part of the solid (150 mg, 0.142 mmol) was chromatographed (Al_2O_3 III, toluene), mixed with CH_2Cl_2 (2.0 mL), recovered with pentane (6.0 mL), washed (pentane; 1:1 ethanol–H_2O solution), vacuum dried (60°C) and weighed (82.5 mg, 42 % based on $SiPc(OH)_2$). UV–vis (DMF) λ_{max}, nm (log ε): 669 (5.32). NMR (300 MHz, $CDCl_3$): δ 9.65 (m, 8H, 1,4-Ar H), 8.34 (m, 8H, 2,3-Ar H), 1.75 (m, 4H, $SiCH_2CH_2CH_2$), −0.84 (m, 4H, $SiCH_2CH_2CH_2$), −2.21 (m, 4H, $SiCH_2CH_2CH_2$), −2.87 (s, 12H, $SiCH_3$). MS–HRFAB (*m/z*): $(M+H)^+$ calculated for $C_{42}H_{41}N_8I_2O_2Si_3$, 1027.0749; found: 1027.0790, 1027.0745.

The compound is a blue solid. It is soluble in toluene, CH_2Cl_2 and DMF and is insoluble in hexanes.

$HOSiPcOSi(CH_3)_2(CH_2)_3I$, ***Pc 58***. A solution of diiodide **Pc 59** (unpurified, 514 mg, 0.488 mmol), trichloroacetic acid (1.64 g, 10.0 mmol) and CH_2Cl_2 (250 mL) was stirred at room temperature for 5 h and then mixed with pyridine (100 mL) and subsequently with H_2O (100 mL). The aqueous layer of this mixture was separated and washed (CH_2Cl_2). The aqueous-layer washings were filtered, and the residue was washed (CH_2Cl_2). The organic layer of the reaction mixture was filtered, and this filtrate, the filtered aqueous-layer washings and the residue washings were combined and evaporated to dryness by rotary evaporation (40°C). The solid was chromatographed (Al_2O_3 V, 1:1 CH_2Cl_2–ethyl acetate solution), mixed with CH_2Cl_2 (4.0 mL), recovered with pentane (12 mL), washed (1:1 ethanol–H_2O solution), vacuum dried (60°C) and weighed (188 mg, 48%). UV–vis (DMF) λ_{max}, nm (log ε): 669 (5.38). NMR (300 MHz, 7.0 m*M*, $CDCl_3$): δ 9.22 (m, 8H, 1,4-Ar H), 8.22 (m, 8H, 2,3-Ar H), 1.59 (m, 2H, $SiCH_2CH_2CH_2$), −1.01 (m, 2H, $SiCH_2CH_2CH_2$), −2.36 (m, 2H, $SiCH_2CH_2CH_2$), −3.04 (s, 6H, $SiCH_3$), −3.22 (s, 1H, SiOH). MS–HRFAB (*m/z*): $(M+H)^+$ calculated for $C_{37}H_{29}N_8IO_2Si_2$, 800.0996; found: 800.0977, 800.1002.

The compound is a blue solid. It is soluble in CH_2Cl_2 and DMF, slightly soluble in toluene and insoluble in hexanes.

$HOSiPcOSi(CH_3)_2(CH_2)_3N(CH_3)(^{14}CH_3)$, ^{14}C–Pc 4. Model synthesis. A stirred suspension of hydroxyiodide **Pc 58** (40.5 mg, 0.0506 mmol), K_2CO_3 (2.4 mg, 0.017 mmol), a solution of $HN(CH_3)_2$ in tetrahydrofuran (2 *M*, 0.2 mL, 0.4 mmol) and tetrahydrofuran (4.8 mL) was warmed (60°C) in a heavy-wall reaction vial for 24 h, and then evaporated to dryness by rotary evaporation (30°C). The solid was mixed with CH_2Cl_2 (4.0 mL), recovered with pentane (16 mL), washed (1:4 CH_2Cl_2–pentane solution; pentane; 1:4 ethanol–H_2O solution), chromatographed (Al_2O_3 III, 10:1 ethyl acetate–methanol solution), washed (pentane; 1:4 ethanol–H_2O solution), vacuum dried (60°C) and weighed (17.5 mg, 48%, 18% based on $SiPc(OH)_2$). Its composition was verified by NMR (34).

^{14}C–Pc 4. With a procedure based on the model synthesis, ^{14}C–Pc 4 was prepared from hydroxyiodide **Pc 58** (450 mg, 0.562 mmol) and $NH(CH_3)(^{14}CH_3)$ by NEN Life Science Products (Boston, MA), (113 mg, 28%). Specific activity (mCi/mmol): 6.33.

CHO cells

The CHO-K1 cell lines were obtained from Dr. Douglas Green (La Jolla, CA) and are designated as 5A100 (CHO) and 5A100-Bcl-2 (CHO-Bcl2), which expresses transfected human Bcl-2. The presence of Bcl-2 was established by Western blot analysis of the protein, using antibody 6C8 (obtained from Dr. Stanley Korsmeyer, Washington University, St. Louis, MO). Cultures were maintained in McCoy's 5A medium containing 10% fetal bovine serum, 100 units/mL penicillin and 100 μg/mL streptomycin at 37°C in a humidified atmosphere with 5% CO_2. The two lines are indistinguishable in morphology and growth rate (doubling time 20–24 h). Experiments were performed on cultures in the exponential phase of growth. Response of the two cell lines to Pc 4–PDT has been reported previously (29,33). For binding assays, the medium was removed from cell cultures in the exponential phase of growth, and the monolayers were washed with phosphate-buffered saline (PBS). The cells were released from the dishes by a brief trypsinization, and the cell pellet (500 ***g,*** 5 min) was washed and resuspended in PBS + 0.1% BSA.

Binding assay

Each preparation was first assayed with 1 n*M* ^{3}H-PK11195 and increasing amounts of protein to establish a concentration that bound 10% of the added ligand (~21 μg of RKM protein and ~2.5×10^5 CHO or CHO-Bcl2 cells), following protocols established by McEnery and coworkers (12,13). For experiments, RKM or CHO cells were incubated with 1 n*M* ^{3}H-PK11195 in the presence or absence of unlabeled PK11195, PPIX or Pc 4 or with ^{14}C–Pc 4 with or without unlabeled PK11195. The final concentration of each ligand is as shown in the figure legends. Reaction mixtures were buffered (TB for RKM and PBS + 0.1% BSA for CHO cells) in a total volume of 200 μL. The standard binding assay of 200 μL was modified for some of the assays because of the relatively low specific radioactivity of the ^{14}C–Pc 4 (1410 dpm/pmol). For analysis of ^{14}C–Pc 4 concentrations lower than 0.5 μ*M*, the total volume of the reaction mixtures was increased to 2.0 mL, maintaining the concentrations of RKM and all other components. For experiments using Pc 4, the reaction mixtures also contained 10% ethanol in the RKM system and 5% ethanol in the CHO cell system. Nonspecific binding of PK11195 was accounted for by subtracting the binding of 1 n*M* ^{3}H-PK11195 in the presence of 100 μ*M* PK11195 from each experimental value. For Pc 4 measures, nonspecific binding was accounted for by subtracting the binding of ^{14}C–Pc 4 alone, without RKM or CHO cells, from each experimental value. The reaction mixtures were incubated on ice for 15 min (RKM) or 1 h (CHO cells). Bound radioactivity was collected on 25 mm glass fiber filters. Filters were air-dried and counted in a Beckman Scintillation Spectrometer. Sigma Plot 4.0 software was used for regression analyses.

Apoptosis in CHO cells

For measurement of apoptosis, CHO cells were plated in 60 mm petri dishes containing three glass coverslips. When the cells were in midlog phase of growth, they were exposed to 0.5 μ*M* Pc 4 with or without the noted concentrations of PK11195 and then returned to the 37°C incubator for 1 h. The cultures were then exposed to approximately equitoxic doses (28) of broad-spectrum red light (λ > 600 nm; 10 kJ/m^2 for CHO cells or 11 kJ/m^2 for CHO-Bcl2 cells) and returned to the 37°C incubator. One coverslip was removed before photoirradiation, and the others at 2 or 4 h after photoirradiation. The cells on the coverslips were fixed in 3.7% formaldehyde for 1 h at room temperature or overnight at 4°C, stained with Hoechst 33342 (1 μg/mL in PBS) for 5 min and examined with a fluorescence microscope for nuclear morphology. For each experimental point, 1000–2000 cells were counted (400×), and apoptotic cells were scored as those with condensed and fragmented nuclei. In order to estimate the number of cells that had detached from the monolayers, the medium was centrifuged at ~2250 ***g*** for 10 min, and the pellet was resuspended in 1 mL of PBS. Cell counts revealed that 1–4% of the control cells were in the medium, and this percentage did not increase when the cells had been treated with PDT, PK11195 or both. Because the floating cell population was small at times up to 4 h after treatment and not dependent on the treatment history, the data presented in the figures reflect only attached cells.

Determination of clonogenicity

Exponential cultures were treated with 0.5 μ*M* Pc 4 with or without 100 μ*M* PK11195, and 1 h later, they were exposed to an approximately LD_{90} fluence (3 kJ/m^2 for CHO and 6 kJ/m^2 for CHO-Bcl2) of red light, as described previously (29). Following the protocol established earlier in the article, after irradiation, some of the cultures were returned to the 37°C incubator for a further 2 h. The cells

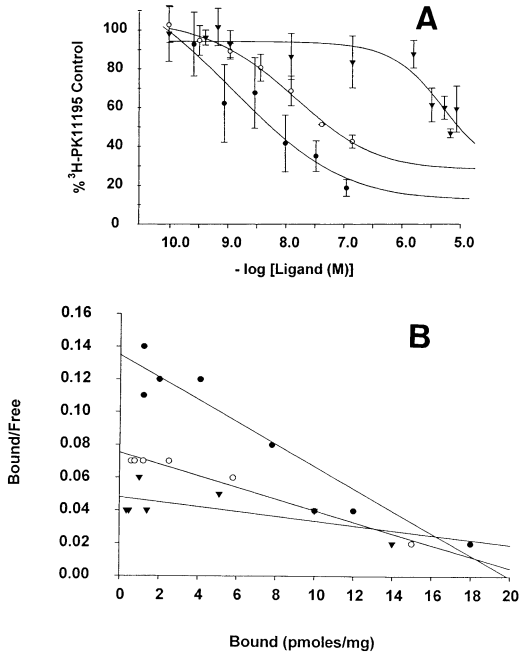

Figure 1. (a) Inhibition of ^{3}H-PK11195 binding to the RKM PBR by unlabeled PK11195 (●), PPIX (○) or Pc 4 (▼). RKM (~22 μg) were incubated with 1 n*M* ^{3}H-PK11195 and increasing concentrations of unlabeled ligand in a total volume of 200 μL of 50 m*M* Tris, 0.1% BSA (TB). For Pc 4, all reaction mixtures contained 10% ethanol. Nonspecific binding was estimated from the binding of ^{3}H-PK11195 in the presence of 10 μ*M* PK11195, and this value was subtracted from each experimental value. Reaction mixtures were incubated on ice for 15 min, and then bound radioactivity was collected on glass fiber filters and counted. The graph represents the mean ± standard deviation of duplicate data for each ligand concentration from three to nine experiments. (b) Scatchard analysis for binding to the RKM PBR by unlabeled PK11195 and the influence of Pc 4. The dose-dependent inhibition of 1 n*M* ^{3}H-PK11195 binding to RKM by unlabeled PK11195 was monitored in the presence of 0 (●), 3 (○) or 5 μ*M* (▼) Pc 4. Reaction mixtures contained 10% ethanol in TB in a total volume of 200 μL. Analyses were conducted as indicated in Fig. 1. Data are from a single experiment reproduced in three to five experiments.

were then released from the monolayers with trypsin, and aliquots were plated into 60 mm petri dishes in amounts sufficient to yield 50–200 colonies per dish. After 12 days of growth, the colonies were stained with 0.1% crystal violet in 20% ethanol, and those with at least 50 cells were counted. The plating efficiency was 44 and 66% for untreated CHO and CHO-Bcl2 cells, respectively. Jurkat cells were treated with an approximately LD_{90} dose of Pc 4–PDT, as estimated from studies with L5178Y-R cells (37,38), and the treatment protocol was followed as mentioned earlier. For determination of clonogenic cell survival, Jurkat cell aliquots were plated into complete medium containing 0.25% BBL agar (Becton Dickinson Microbiology Systems, Sparks, MD), and the colonies were counted after 12–14 days.

RESULTS

Inhibition of ^{3}H-PK11195 binding to the RKM PBR

Figure 1a presents data for the inhibition of 1 n*M* ^{3}H-PK11195 binding to the RKM PBR by unlabeled PK11195, PPIX or Pc 4. In accordance with reported literature, we confirmed a concentration-dependent inhibition of ^{3}H-PK11195 binding to RKM by unlabeled PK11195 or by PPIX and found similar IC_{50} values (concentrations causing 50% inhibition of binding of ^{3}H-PK11195) for these ligands (Table 1). It should be noted that all reaction mixtures contained 0.1% BSA to stabilize the mitochondria as well as to prevent the precipitation of hydrophobic ligands. BSA is known to have a binding site for isoquinoline carboxamides and thus might compete for binding of PK11195 with sites on RKM. The similarity of binding parameters in our experiments to literature values (Table 1) suggests that any competition by BSA is relatively minor.

Table 1. Summary of binding constants for the interaction of PK11195, PPIX and Pc 4 to PBR of isolated RKM

	IC_{50}	
Ligand	This study*	Verma *et al.* (23)
PK11195	3 n*M*	1.5 ± 0.4 n*M*
PPIX	30 n*M*	27 ± 5.6 n*M*
Pc 4	3 μ*M*	ND‡

	K_d and B_{max}		
	This study†	Verma *et al.* (23)	Hirsch *et al.* (63)
K_d (n*M*)	6.3	3	6.6
B_{max} (pmole/mg)	7.6	13	5.1

*From Fig. 1.
†Not shown.
‡Not determined.

Analysis of Pc 4 inhibition of ^{3}H-PK11195 binding required that an appropriate solvent mixture first be selected. Pc 4 is a large, planar aromatic compound that is not soluble in water and tends to aggregate in aqueous solutions. As noted in the earlier paragraph, aggregation and precipitation was reduced by BSA in the reaction mixtures. To further promote Pc 4 solubility, the binding of ^{3}H-PK11195 to RKM PBR was tested in various levels of DMF and ethanol. The system tolerated a 10% ethanol solution in TB without interference of ^{3}H-PK11195 binding, as revealed by the absence of significant changes in B_{max} or K_d. All assays of Pc 4 were thus conducted in a solution containing 10% ethanol in TB. In contrast, the benzodiazepine site on the PBR, often assessed through binding of Ro5-4864, was not stable in the presence of 10% ethanol and thus could not be evaluated under these conditions (data not shown).

Figure 1a reveals that inhibition of ^{3}H-PK11195 binding to the RKM PBR was extensive at Pc 4 concentrations at or above 1 μ*M*, whereas a modest effect was observed at lower concentrations (10^{-6}–10^{-9} *M*), inhibiting up to approximately 20% of the PK11195-binding sites. No significant inhibition of ^{3}H-PK11195 binding was observed at Pc 4 concentrations ≤1 n*M*. No significant change in the Pc 4 absorption spectrum was found in the presence of 100 μ*M* PK11195, consistent with an absence of direct interaction between these two compounds (data not shown).

To determine if Pc 4 was behaving as a competitive inhibitor of PK11195 for binding to the PBR, the dose-dependent inhibition of 1 n*M* ^{3}H-PK11195 binding to the RKM PBR by unlabeled PK11195 was measured in the presence of 0, 3 or 5 μ*M* Pc 4 (Fig. 1b). In the absence of Pc 4, the B_{max} and the K_d values for PK11195 binding to the RKM

Scheme 1.

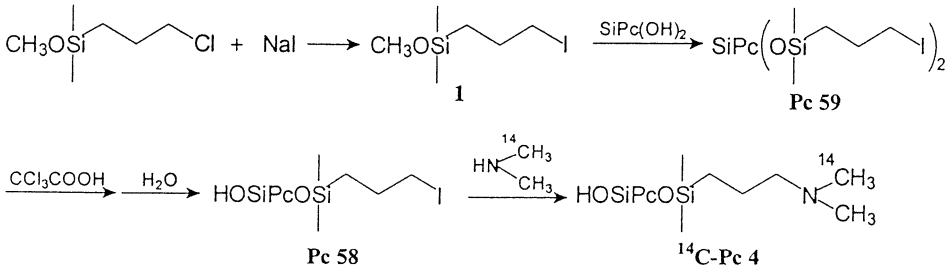

PBR were similar to literature values (Table 1). Scatchard analysis shows three curves intersecting at a point near the abscissa, with slopes that decrease as the Pc 4 concentration increases. The combined data are consistent with competition by Pc 4 with PK11195 for binding to the RKM PBR.

Synthesis of ^{14}C–Pc 4

The route to Pc 4 used in the model synthesis section for ^{14}C–Pc 4 is less convenient than an earlier improved route to it (39). Further, it gives a lower yield (18 *vs* 83% based on $SiPc(OH)_2$) and a lower purity (94 *vs* 98%). Nevertheless, the route is well suited to the synthesis of ^{14}C–Pc 4 (Scheme 1, Fig. 2) because the $^{14}CH_3$ group is added in a step that is simple, clean and at the end of the route.

Pc 4 binding to RKM and the effect of PK11195

To further investigate the nature of the competition between PK11195 and Pc 4, we measured ^{14}C–Pc 4 binding to RKM in the presence or absence of unlabeled PK11195. In the range of 0.5–10 μ*M* Pc 4 (Fig. 3a), the characteristics of ^{14}C–Pc 4 binding to RKM were markedly different from those for PK11195 binding. First, there was a linear dose-dependent increase in ^{14}C–Pc 4 binding to the RKM, with no evidence of saturation. Second, the binding of ^{14}C–Pc 4, even at concentrations as low as 25 n*M* (Fig. 3b), was not inhibited in the presence of high saturating levels of PK11195.

PBR parameters in CHO cells

In order to assess the relevance of the RKM studies to cells in culture that can be photoinactivated by Pc 4 and light (28), binding studies were conducted using intact CHO cells. For analysis of Pc 4 binding, the reaction mixtures contained 5% ethanol, which did not affect the binding parameters of PK11195 in CHO cells. As in the RKM system, a PK11195 concentration–dependent inhibition of ^{3}H-PK11195 binding to CHO cells was observed, and an IC_{50} of 40 n*M* was found (data not shown), a value similar to earlier reports (40,41). For Pc 4, however, concentrations ≤1 μ*M* were not inhibitory to ^{3}H-PK11195 binding, whereas the low-affinity Pc 4–binding site, established in RKM, was observed at micromolar concentrations (Fig. 4a,b). When ^{14}C–Pc 4 binding to CHO cells was measured in the presence or absence of unlabeled PK11195 (Fig. 4c,d), the results reflected those found in the RKM system. A linear dose-dependent increase in ^{14}C–Pc 4 binding to the CHO cells was observed, with no

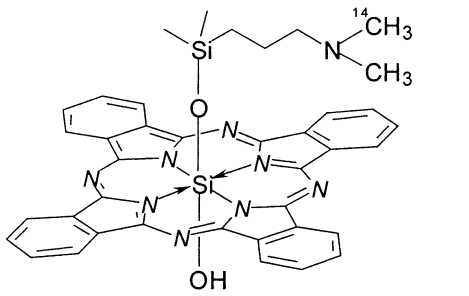

Figure 2. Structure of ^{14}C–Pc 4.

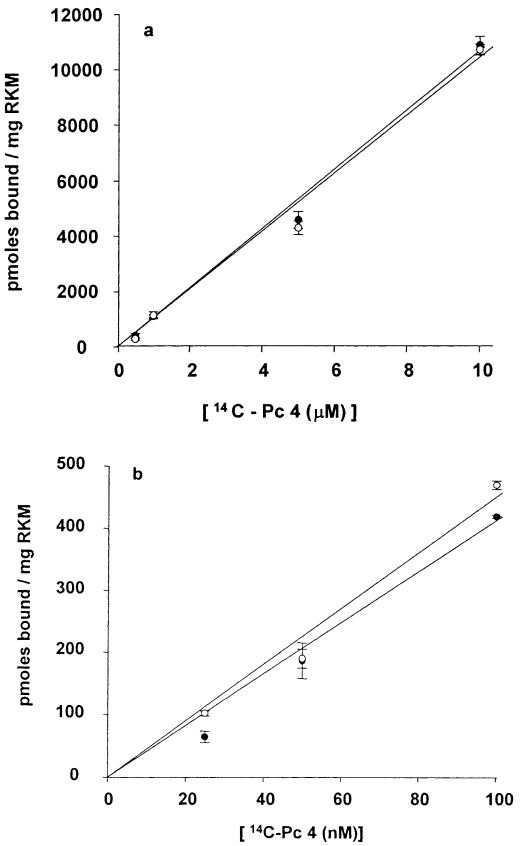

Figure 3. Binding of ^{14}C–Pc 4 to the RKM. RKM were incubated with increasing concentrations of ^{14}C–Pc 4, as indicated on the abscissa, with (○) or without (●) 10 μ*M* PK11195, in 10% ethanol in TB. For (a), the standard reaction volume of 200 μL contained 0.5–10 μ*M* ^{14}C–Pc 4. For (b), the reaction volume was increased to 2 mL in order to assay lower concentrations of ^{14}C–Pc 4 (25–100 n*M*). The concentrations of RKM and all other components were kept constant. Analysis of bound radioactivity was as for Fig. 1. Nonspecific binding was accounted for by subtracting the binding of ^{14}C–Pc 4 without RKM from each experimental value. Data are indicated as the mean ± standard deviation from duplicate data of one representative experiment.

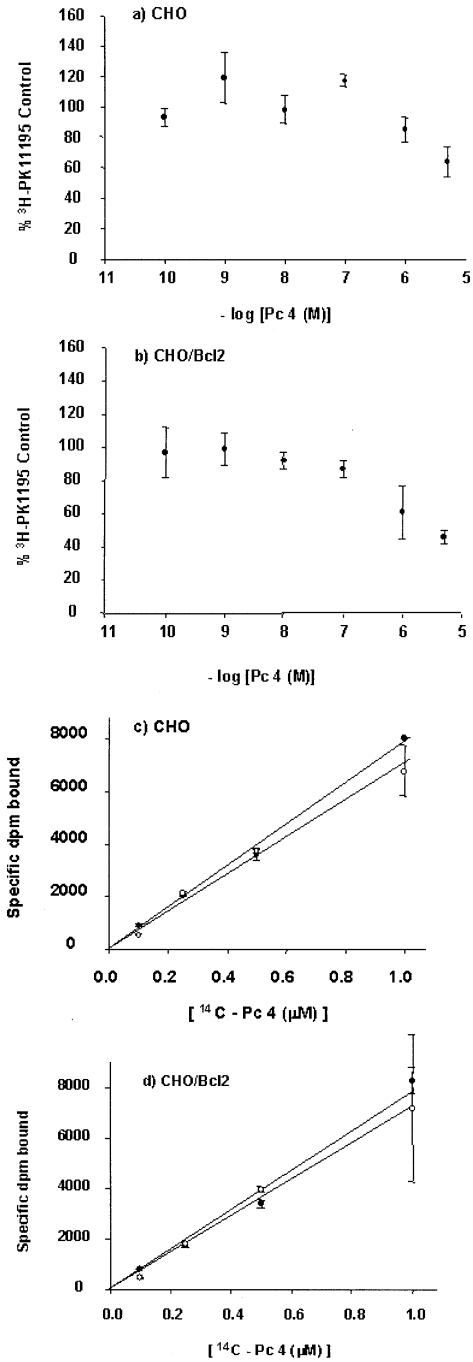

Figure 4. Inhibition of ^{3}H-PK11195 binding by Pc 4 to PBR of (a) CHO cells and (b) CHO-Bcl2 cells. CHO cells (~2.5 × 10^{5} cells) were incubated with 1 n*M* ^{3}H-PK11195 and increasing concentrations of unlabeled ligand in a total volume of 200 μL of PBS + 0.1% BSA. For Pc 4, all reaction mixtures contained 5% ethanol. Reaction mixtures were incubated on ice for 1 h and the analysis of bound radioactivity followed as in Fig. 1. The plot shown is a representative trial from a series of two to four trials. Data are indicated as the mean ± standard deviation. Binding of ^{14}C–Pc 4 to the CHO cells (c) and CHO-Bcl2cells (d). CHO cells were incubated with increasing concentrations of ^{14}C–Pc 4, as shown on the abscissa, with (○) or without (●) 10 μ*M* PK11195, in 5% ethanol in PBS + 0.1% BSA in a total volume of 2 mL. Analysis of bound radioactivity was as for Fig. 1. Data shown in the graph are the mean ± standard deviation from duplicate data of one representative experiment.

evidence for saturation up to 1 μ*M*. Again, high saturating levels of PK11195 did not inhibit the binding of ^{14}C–Pc 4 to the CHO cells. Furthermore, there were no marked differences in the binding of ^{14}C–Pc 4 to the two CHO cell lines.

PBR interactions affect Pc 4–PDT

PBR is presumed to function as part of PTPC, and previous studies have shown that addition of PK11195 to cells can either prevent (42) or promote (43) apoptosis by different agents. Because we found evidence for the binding of Pc 4 to PBR, and Pc 4–PDT is a strong inducer of apoptosis, we asked if PK11195 could affect the ability of Pc 4–PDT–treated cells to undergo apoptosis. For this study, we used CHO cells and a companion cell line that overexpresses human Bcl-2 and is made partially resistant to Pc 4–PDT by Bcl-2 (29). Pc 4 or PK11195, or the two compounds together, did not have any effect on cell morphology or growth rate in the absence of light, and PK11195 plus the Pc 4–activating red light was also without effect (data not shown). Cells were treated with PDT (0.5 μ*M* Pc 4 + 10 kJ/m^{2} for CHO or 11 kJ/m^{2} for CHO-Bcl2) in the presence or absence of 0.1–100 μ*M* PK11195 (Fig. 5). As shown in Fig. 5a, PDT induced rapid apoptosis in CHO cells, involving nearly 100% of the cells by 4 h after photoirradiation. Apoptosis was also induced in the cells expressing transfected Bcl-2 (Fig. 5b), but the process was slower and less extensive, confirming that equitoxic doses in terms of clonogenicity do not lead to equal levels of apoptosis. In both cell lines, PK11195 strongly inhibited apoptosis. However, the effect of PK11195 appears to be transient because there was increased apoptosis in PK11195-treated cells at 4 h in comparison with 2 h post-PDT, and the effect of PK11195 at 4 h was not statistically significant.

Clonogenicity of CHO and CHO-Bcl2 cells after PDT ± PK11195

Because apoptosis may be the mechanism of cell removal for only part of the PDT-killed cells, cell death was also determined by a clonogenic assay. Cells were treated with an approximately LD_{90} dose (29) of PDT (0.5 μ*M* Pc 4 + 3 or 6 kJ/m^{2} of red light for CHO or CHO-Bcl2 cells, respectively), with or without 100 μ*M* PK11195 under the same culture conditions as those used for the assay for apoptosis of Fig. 5. After treatments, cell monolayers were recovered, either immediately after PDT (0 h) or after a 2 h post-PDT incubation at 37°C, and suitable aliquots were plated to determine the clonogenic survival. The results (Fig. 6) show that the clonogenic survival for both cell lines was very close to the level expected on the basis of previous results; *i.e.* about 20% survival compared with 10% survival determined earlier (29). For both cell lines, the survival level did not change on delaying cell recovery and plating to 2 h after PDT, suggesting the absence of potentially lethal damage repair in these cells. CHO cells, but not CHO-Bcl2 cells, were partially protected from cell death by 100 μ*M* PK11195, and the PBR ligand was nontoxic in the absence of PDT. The protection of CHO cells was reduced when recovery of the cells was delayed for 2 h after PDT.

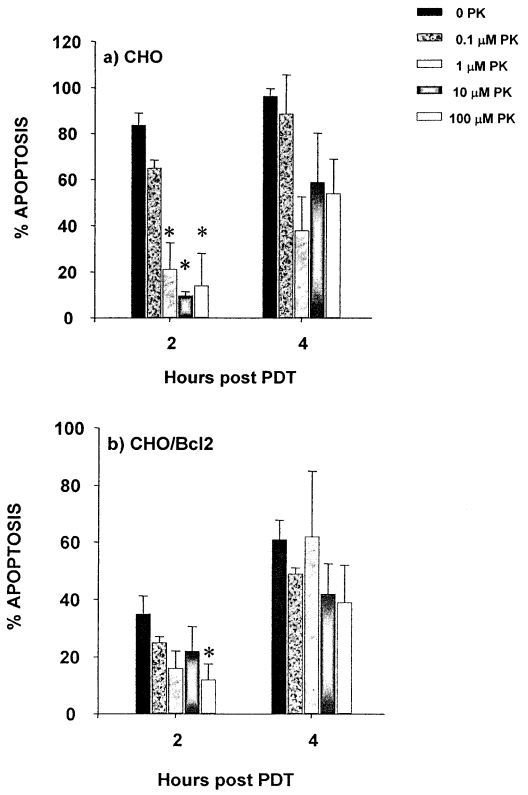

Figure 5. The induction of apoptosis by Pc 4–PDT and the effect of PK11195. (a) CHO or (b) CHO-Bcl2cells were plated in 60 mm petri dishes containing three glass coverslips. When the cells were in midlog phase of growth, the cultures received 0.5 μ*M* Pc 4 with or without the noted concentrations of PK11195, and 1 h later, they were exposed to approximately equitoxic doses of broad-spectrum red light ($\lambda > 600$ nm; 10 kJ/m^2 for a and 11 kJ/m^2 in b) and returned to the 37°C incubator. One coverslip from each dish was removed before photoirradiation, and the others were removed at 2 or 4 h after photoirradiation. The cells on the coverslips were fixed, stained with Hoechst 33342 and examined with a fluorescence microscope for nuclear morphology. Each bar represents the mean ± standard deviation of the data from 1000–2000 cells per experimental point (*, $P < 0.05$).

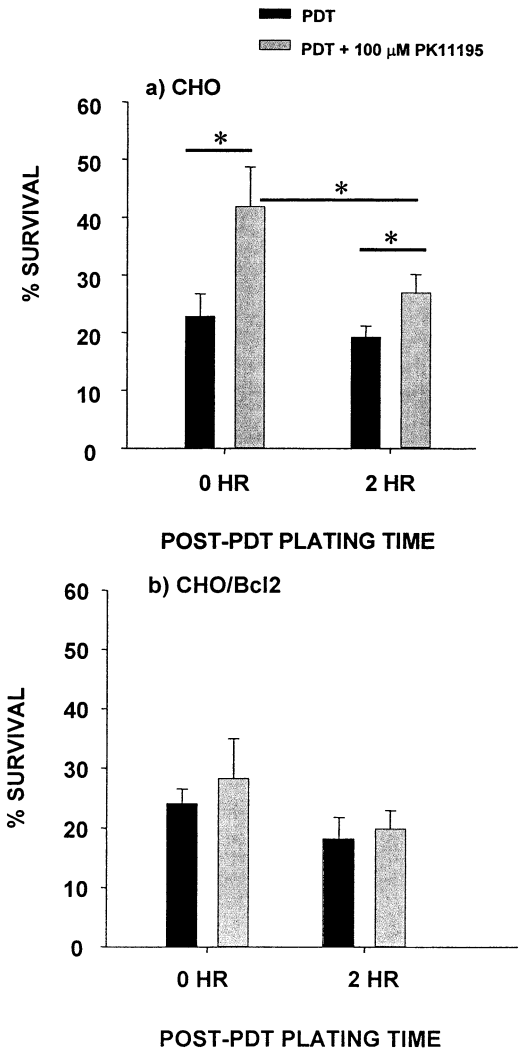

Figure 6. Clonogenic survival of (a) CHO or (b) CHO-Bcl2 cells treated with Pc 4–PDT ± 100 μ*M* PK11195. Cells were treated with an approximate LD_{90} dose (29) of PDT (0.5 μ*M* Pc 4 + 3 or 6 kJ/m^2 of red light for CHO or CHO-Bcl2 cells, respectively), with or without 100 μ*M* PK11195, under the same culture conditions as those used for the assay of apoptosis. After treatments, cell monolayers were recovered, either immediately after PDT (0 h) or after a 2 h post-PDT incubation at 37°C, and suitable aliquots were plated to determine the clonogenic survival. Each bar indicates the mean ± standard error of five to six values per experimental point. The horizontal lines indicate the data sets that were compared by *t*-test and found to be significant (*, $P < 0.05$).

Effect of PK11195 in Jurkat cells

Because Jurkat cells do not express PBR (44), we exploited this feature to investigate the PBR-independent effects of PK11195. Confirming the results of Bono *et al.* (44), we found no binding of ^{3}H-PK11195 to those cells (data not shown). However, a high level of PK11195 (100 μ*M*) was toxic to Jurkat cells, reducing clonogenic survival to 32% after a 2 h exposure. Because of the toxicity, we have not studied interactive effects with PDT in these cells.

DISCUSSION

PBR is a ubiquitous receptor, implicated in housekeeping functions of cellular metabolism, neuroendocrine activity and immune function (17). The highest levels of PBR are found in tissues with high metabolic activity, especially rapid oxidative phosphorylation (45). Upregulation of PBR has been observed in tumors, including breast, liver, endometrium, ovary and prostate (46–51). Recently, PBR expression has also been correlated to an aggressive phenotype and proliferation of some breast cancer cell lines (52–55). High levels of PBR expression also correlated with resistance to hydrogen peroxide cytotoxicity (56).

Regarding PBR ligand-binding properties in apoptosis, however, studies remain inconclusive. In cell lines of lymphoid origin, PK11195 has previously been reported to promote induction of apoptosis by glucocorticoids, etoposide, ionizing radiation, lonidamine and arsenite (43,57,58). In contrast, Bono *et al.* (44) showed that the binding affinity of several PBR ligands was positively correlated with their antiapoptotic potential in TNF-α–treated U937 cells.

Miccoli *et al.* (59) determined that exposing human glioma cells to PK11195 for 24 h caused an increase in mitochondrial membrane fluidity and in parameters associated

with cell growth and DNA synthesis. Although the longest exposure of CHO cells to PK11195 in our studies was 5 h, it is possible that one effect of the ligand was to alter membrane fluidity and thus either the interaction of PBR sites with other ligands or with other mitochondrial proteins.

The present study identified substantial low-affinity binding of Pc 4 to the RKM PBR, as observed at concentrations ≥ 1 μM, and possibly limited higher-affinity binding. Nevertheless, data with CHO cells support the presence of only the low-affinity sites. Two populations of binding sites, if truly present, could reflect a dynamic interplay between the 18 kDa protein in the free state or in a complex with other mitochondrial membrane proteins that affect drug specificity and physiology. Previous reports have identified multiple isoforms of PBR, displaying both high and low affinity for PK11195, in rat liver preparations (60). However, because significant interaction of Pc 4 with PBR was found only at concentrations ≥ 1 μM, PBR is unlikely to be a major binding site for Pc 4 under conditions normally employed for *in vitro* PDT experiments, which utilize 20–500 n*M* Pc 4. Furthermore, although the presence of ethanol did not alter the parameters of binding of PK11195 to its site on the PBR, it did interfere with the benzodiazepine site, as monitored with Ro5-4864. If Pc 4 has greater affinity for that site than for the PK11195 site, our ability to observe that interaction would have been compromised by the reaction conditions.

Although Pc 4 competed with ^{3}H-PK11195 for binding to the PBR of RKM, the reciprocal assay found ^{14}C–Pc 4 binding to be unaffected by even a high saturating level (10 μM) of PK11195. Notably, relatively high concentrations of Pc 4 were required for competition with PK11195 for its binding site on the RKM PBR and on the PBR of CHO cells. Further, the binding of ^{14}C–Pc 4 to RKM showed no tendency to reach saturation, arguing that Pc 4 binds to multiple sites on mitochondria in addition to those associated with PBR. These observations support a model in which the binding sites for PK11195 and a subset of those for Pc 4 on the PBR are not identical but may be related. One possible mitochondrial site for binding of Pc 4 is likely to be at or near the site of interaction of the antiapoptotic protein Bcl-2 to the mitochondrial outer membrane because Xue *et al.* (33) and others (61) have demonstrated that Pc-based PDT causes immediate direct photodamage to Bcl-2. Nevertheless, to date, there is no evidence for direct interaction of Bcl-2 and the PBR.

In a study of the possible role of PBR in PDT-induced apoptosis in CHO cells, PK11195 was found to inhibit Pc 4–PDT–induced apoptosis both in Bcl-2–transfected and in control CHO cell lines. These results contrast with those of Hirsch *et al.* (43), who showed that PK11195 could overcome the antiapoptotic effects of Bcl-2 after treatment with a variety of (non-PDT) apoptosis-inducing agents. In the case of Pc 4–PDT, however, PK11195 prevented apoptosis whether or not the cells overexpressed Bcl-2. Based on our finding that both endogenous and overexpressed Bcl-2 of these CHO cells are extensively photodamaged by Pc 4–PDT (33), it is not surprising that the inhibition of apoptosis by PK11195 would occur irrespective of the initial level of intact Bcl-2. Our results showing a short-term inhibition of apoptosis are in accordance with those of Ratcliffe and Matthews (42), who also used a short-term assay (tetrazolium dye reduction) in a study of PDT on rat pancreatoma cells photosensitized by PPIX generated from exogenously supplied δ-aminolevulinic acid. Neither did they study the influence of Bcl-2 on the process nor did they confirm the results of the short-term assay by measuring clonogenicity. Further work is needed to ascertain whether or not the effects of PK11195 are specific to initial photosensitizer-dependent reactions at the PBR or whether other PBR-mediated steps in apoptosis may be blocked. In addition, because the PBR has been localized to other organelles, including the nuclear envelope (54) and the plasma membrane (62), the effects of other PK11195-binding sites on the observed inhibition of apoptosis cannot be excluded. In fact, the toxicity of PK11195 to PBR-null Jurkat cells is consistent with the ability of this ligand to interact with other cellular targets.

Although PK11195 provides a marked inhibition of apoptosis early (2 h) after PDT, the inhibition was less pronounced by 4 h post-PDT, indicating that it is transient. This suggests that the inhibition of apoptosis does not affect the generation of lethal damage by Pc 4–PDT. This presumption was largely confirmed by clonogenic assays, which demonstrated only a modest effect of PK11195 on overall cell death in CHO cells. In CHO-Bcl2 cells, PK11195 did not alter the ability of Pc 4–PDT to produce lethal damage. The data may indicate that PK11195 and Bcl-2 are influencing the same series of reactions leading to cell death.

In conclusion, PBR is proposed as the primary target for photodamage induced by some (26) but not all (27) porphyrin-derived photosensitizers. The current study suggests that Pc 4 may exert some of its photodynamic damage *via* binding to PBR but that the low affinity for Pc 4 at the observed sites is not consistent with a biologically significant role for PBR in Pc 4 binding to the mitochondria. Additional mitochondrial targets of Pc 4–PDT, including Bcl-2, are likely.

Acknowledgements—This research was supported by the U.S. Public Health Service Grants P01 CA48735, R01 CA83917 and P30 CA43703 from the National Cancer Institute, DHHS.

REFERENCES

1. Dougherty, T. J., C. J. Gomer, B. W. Henderson, G. Jori, D. Kessel, M. Korbelik, J. Moan and Q. Peng (1998) Photodynamic therapy. *J. Natl. Cancer Inst.* **90**, 889–905.
2. Dougherty, T. J. and S. L. Marcus (1992) Photodynamic therapy. *Eur. J. Cancer* **10**, 1734–1742.
3. Kessel, D. and Y. Luo (1998) Mitochondrial photodamage and PDT-induced apoptosis. *J. Photochem. Photobiol. B: Biol.* **42**, 89–95.
4. Varnes, M. E., S. M. Chiu, L. Y. Xue and N. L. Oleinick (1999) Photodynamic therapy-induced apoptosis in lymphoma cells: translocation of cytochrome *c* causes inhibition of respiration as well as caspase activation. *Biochem. Biophys. Res. Commun.* **255**, 673–679.
5. Oleinick, N. L. and H. H. Evans (1998) The photobiology of photodynamic therapy: cellular targets and mechanisms. *Radiat. Res.* **150**, S146–S156.
6. Moor, A. C. (2000) Signaling pathways in cell death and survival after photodynamic therapy. *J. Photochem. Photobiol. B: Biol.* **57**, 1–13.
7. Oleinick, N. L., R. L. Morris and I. Belichenko (2002) Apoptosis in response to photodynamic therapy: what, where, why, and how? *Photochem. Photobiol. Sci.* **1**, 1–21.
8. Adrain, C. and S. J. Martin (2001) The mitochondrial apoptosome: a killer unleashed by the cytochrome seas. *Trends Biochem. Sci.* **26**, 390–397.
9. Xue, L. Y., S. M. Chiu and N. L. Oleinick (2001) Photodynamic

therapy-induced death of MCF-7 human breast cancer cells: a role for caspase-3 in the late steps of apoptosis but not for the critical lethal event. *Exp. Cell Res.* **263**, 145–155.
10. Costantini, P., E. Jacotot, D. Decaudin and G. Kroemer (2000) Mitochondrion as a novel target of anticancer chemotherapy. *J. Natl. Cancer Inst.* **92**, 1042–1053.
11. Loeffler, M. and G. Kroemer (2000) The mitochondrion in cell death control: certainties and incognita. *Exp. Cell Res.* **256**, 19–26.
12. McEnery, M. W. (1992) The mitochondrial benzodiazepine receptor: evidence for association with the voltage-dependent anion channel (VDAC). *J. Bioenerg. Biomembr.* **24**, 63–69.
13. McEnery, M. W., A. M. Snowman, R. R. Trifiletti and S. H. Snyder (1992) Isolation of the mitochondrial benzodiazepine receptor: association with the voltage-dependent anion channel and the adenine nucleotide carrier. *Proc. Natl. Acad. Sci. USA* **89**, 3170–3174.
14. Kinnally, K. W., D. B. Zorov, Y. N. Antonenko, S. H. Snyder, M. W. McEnery and H. Tedeschi (1993) Mitochondrial benzodiazepine receptor linked to inner membrane ion channels by nanomolar actions of ligands. *Proc. Natl. Acad. Sci. USA* **90**, 1374–1378.
15. Jimenez, A., D. Pubill, M. Pallas, A. Camins, S. Llado, J. Camarasa and E. Escubedo (2000) Further characterization of an adenosine transport system in the mitochondrial fraction of rat testis. *Eur. J. Pharmacol.* **398**, 31–39.
16. Brown, R. C. and V. Papadopoulos (2001) Role of the peripheral-type benzodiazepine receptor in adrenal and brain steroidogenesis. *Int. Rev. Neurobiol.* **46**, 117–143.
17. Gavish, M., I. Bachman, R. Shoukrun, Y. Katz, L. Veenman, G. Weisinger and A. Weizman (1999) Enigma of the peripheral benzodiazepine receptor. *Pharmacol. Rev.* **51**, 629–650.
18. Papadopoulos, V. (1998) Structure and function of the peripheral-type benzodiazepine receptor in steroidogenic cells. *Proc. Soc. Exp. Biol. Med.* **217**, 130–142.
19. Papadopoulos, V. and A. S. Brown (1995) Role of the peripheral-type benzodiazepine receptor and the polypeptide diazepam binding inhibitor in steroidogenesis. *J. Steroid Biochem. Mol. Biol.* **53**, 103–110.
20. Taketani, S., H. Kohno, T. Furukawa and R. Tokunaga (1995) Involvement of peripheral-type benzodiazepine receptors in the intracellular transport of heme and porphyrins. *J. Biochem. (Tokyo)* **117**, 875–880.
21. Snyder, S. H., A. Verma and R. R. Trifiletti (1987) The peripheral-type benzodiazepine receptor: a protein of mitochondrial outer membranes utilizing porphyrins as endogenous ligands. *Faseb J.* **1**, 282–288.
22. Verma, A., J. S. Nye and S. H. Snyder (1987) Porphyrins are endogenous ligands for the mitochondrial (peripheral-type) benzodiazepine receptor. *Proc. Natl. Acad. Sci. USA* **84**, 2256–2260.
23. Verma, A. and S. H. Snyder (1988) Characterization of porphyrin interactions with peripheral type benzodiazepine receptors. *Mol. Pharmacol.* **34**, 800–805.
24. Verma, A. and S. H. Snyder (1989) Peripheral type benzodiazepine receptors. *Annu. Rev. Pharmacol. Toxicol.* **29**, 307–322.
25. Snyder, S. H., M. W. McEnery and A. Verma (1990) Molecular mechanisms of peripheral benzodiazepine receptors. *Neurochem. Res.* **15**, 119–123.
26. Verma, A., S. L. Facchina, D. J. Hirsch, S. Y. Song, L. F. Dillahey, J. R. Williams and S. H. Snyder (1998) Photodynamic tumor therapy: mitochondrial benzodiazepine receptors as a therapeutic target. *Mol. Med.* **4**, 40–45.
27. Kessel, D., M. Antolovich and K. M. Smith (2001) The role of the peripheral benzodiazepine receptor in the apoptotic response to photodynamic therapy. *Photochem. Photobiol.* **74**, 346–349.
28. Potter, W. R., B. W. Henderson, D. A. Bellnier, R. K. Pandey, L. A. Vaughan, K. R. Weishaupt and T. J. Dougherty (1999) Parabolic quantitative structure–activity relationships and photodynamic therapy: application of a three-compartment model with clearance to the *in vivo* quantitative structure–activity relationships of a congeneric series of pyropheophorbide derivatives used as photosensitizers for photodynamic therapy. *Photochem. Photobiol.* **70**, 781–788.
29. He, J., M. L. Agarwal, H. E. Larkin, L. R. Friedman, L. Y. Xue and N. L. Oleinick (1996) The induction of partial resistance to photodynamic therapy by the protooncogene BCL-2. *Photochem. Photobiol.* **64**, 845–852.
30. He, J., C. M. Whitacre, L. Y. Xue, N. A. Berger and N. L. Oleinick (1998) Protease activation and cleavage of poly(ADP-ribose) polymerase: an integral part of apoptosis in response to photodynamic treatment. *Cancer Res.* **58**, 940–946.
31. Trivedi, N. S., H. W. Wang, A. L. Nieminen, N. L. Oleinick and J. A. Izatt (2000) Quantitative analysis of Pc 4 localization in mouse lymphoma (LY-R) cells *via* double-label confocal fluorescence microscopy. *Photochem. Photobiol.* **71**, 634–639.
32. Lam, M., N. L. Oleinick and A. L. Nieminen (2001) Photodynamic therapy-induced apoptosis in epidermoid carcinoma cells: reactive oxygen species and mitochondrial inner membrane permeabilization. *J. Biol. Chem.* **276**, 47379–47386.
33. Xue, L. Y., S. M. Chiu and N. L. Oleinick (2001) Photochemical destruction of the Bcl-2 oncoprotein during photodynamic therapy with the phthalocyanine photosensitizer Pc 4. *Oncogene* **20**, 3420–3427.
34. Oleinick, N. L., A. R. Antunez, M. E. Clay, B. D. Rihter and M. E. Kenney (1993) New phthalocyanine photosensitizers for photodynamic therapy. *Photochem. Photobiol.* **57**, 242–247.
35. Lowry (1951) Protein measurement with the Folin reagent. *J. Biol. Chem.* **193**, 265–275.
36. Rickwood, D. and A. Hayes (1984) An evaluation of methods used to prepare yeast mitochondria for transcriptional studies. *Prep. Biochem.* **14**, 163–171.
37. Evans, H. H., M. F. Horng, M. Ricanati and E. C. McCoy (1999) Differential antimutagenicity of WR-1065 added after irradiation in L5178Y cell lines. *Radiat. Res.* **151**, 391–397.
38. Chiu, S., H. H. Evans, M. Lam, A. Nieminen and N. L. Oleinick (2001) Phthalocyanine 4 photodynamic therapy-induced apoptosis of mouse L5178Y- R cells results from a delayed but extensive release of cytochrome *c* from mitochondria. *Cancer Lett.* **165**, 51–58.
39. Li, Y. S. and M. E. Kenney (1998) Novel methods of synthesis of phthalocyanine compounds. U.S. Patent 5,763,602. June 9, 1998 [also PCT Int. Appl. WO 9814521 A1, April 9, 1998].
40. Riond, J., M. G. Mattei, M. Kaghad, X. Dumont, J. C. Guillemot, G. Le Fur, D. Caput and P. Ferrara (1991) Molecular cloning and chromosomal localization of a human peripheral-type benzodiazepine receptor. *Eur. J. Biochem.* **195**, 305–311.
41. Riond, J., N. Vita, G. Le Fur and P. Ferrara (1989) Characterization of a peripheral-type benzodiazepine-binding site in the mitochondria of Chinese hamster ovary cells. *FEBS Lett.* **245**, 238–244.
42. Ratcliffe, S. L. and E. K. Matthews (1995) Modification of the photodynamic action of delta-aminolaevulinic acid (ALA) on rat pancreatoma cells by mitochondrial benzodiazepine receptor ligands. *Br. J. Cancer* **71**, 300–305.
43. Hirsch, T., D. Decaudin, S. A. Susin, P. Marchetti, N. Larochette, M. Resche-Rigon and G. Kroemer (1998) PK11195, a ligand of the mitochondrial benzodiazepine receptor, facilitates the induction of apoptosis and reverses Bcl-2-mediated cytoprotection. *Exp. Cell Res.* **241**, 426–434.
44. Bono, F., I. Lamarche, V. Prabonnaud, G. Le Fur and J. M. Herbert (1999) Peripheral benzodiazepine receptor agonists exhibit potent antiapoptotic activities. *Biochem. Biophys. Res. Commun.* **265**, 457–461.
45. Hirsch, J. D., C. F. Beyer, L. Malkowitz, B. Beer and A. J. Blume (1989) Mitochondrial benzodiazepine receptors mediate inhibition of mitochondrial respiratory control. *Mol. Pharmacol.* **35**, 157–163.
46. Batra, S. and J. Alenfall (1994) Characterization of peripheral benzodiazepine receptors in rat prostatic adenocarcinoma. *Prostate* **24**, 269–278.
47. Batra, S. and C. S. Iosif (1998) Elevated concentrations of mitochondrial peripheral benzodiazepine receptors in ovarian tumors. *Int. J. Oncol.* **12**, 1295–1298.
48. Batra, S., I. Larsson and E. Boven (2000) Mitochondrial and microsomal peripheral benzodiazepine receptors in human ovarian cancer xenografts. *Int. J. Mol. Med.* **5**, 619–623.
49. Beinlich, A., R. Strohmeier, M. Kaufmann and H. Kuhl (1999)

Specific binding of benzodiazepines to human breast cancer cell lines. *Life Sci.* **65**, 2099–2108.
50. Venturini, I., M. L. Zeneroli, L. Corsi, R. Avallone, F. Farina, H. Alho, C. Baraldi, C. Ferrarese, N. Pecora, M. Frigo, G. Ardizzone and A. Arrigo (1998) Up-regulation of peripheral benzodiazepine receptor system in hepatocellular carcinoma. *Life Sci.* **63**, 1269–1280.
51. Venturini, I., H. Alho, I. Podkletnova, L. Corsi, E. Rybnikova, R. Pellicci, M. Baraldi, M. Pelto-Huikko, P. Helen and M. L. Zeneroli (1999) Increased expression of peripheral benzodiazepine receptors and diazepam binding inhibitor in human tumors sited in the liver. *Life Sci.* **65**, 2223–2231.
52. Beinlich, A., R. Strohmeier, M. Kaufmann and H. Kuhl (2000) Relation of cell proliferation to expression of peripheral benzodiazepine receptors in human breast cancer cell lines. *Biochem. Pharmacol.* **60**, 397–402.
53. Carmel, I., F. A. Fares, S. Leschiner, H. Scherubl, G. Weisinger and M. Gavish (1999) Peripheral-type benzodiazepine receptors in the regulation of proliferation of MCF-7 human breast carcinoma cell line. *Biochem. Pharmacol.* **58**, 273–278.
54. Hardwick, M., D. Fertikh, M. Culty, H. Li, B. Vidic and V. Papadopoulos (1999) Peripheral-type benzodiazepine receptor (PBR) in human breast cancer: correlation of breast cancer cell aggressive phenotype with PBR expression, nuclear localization, and PBR-mediated cell proliferation and nuclear transport of cholesterol. *Cancer Res.* **59**, 831–842.
55. Sanger, N., R. Strohmeier, M. Kaufmann and H. Kuhl (2000) Cell cycle-related expression and ligand binding of peripheral benzodiazepine receptor in human breast cancer cell lines. *Eur. J. Cancer* **36**, 2157–2163.
56. Carayon, P., M. Portier, D. Dussossoy, A. Bord, G. Petitpretre, X. Canat, G. Le Fur and P. Casellas (1996) Involvement of peripheral benzodiazepine receptors in the protection of hematopoietic cells against oxygen radical damage. *Blood* **87**, 3170–3178.
57. Ravagnan, L., I. Marzo, P. Costantini, S. A. Susin, N. Zamzami, P. X. Petit, F. Hirsch, M. Goulbern, M. F. Poupon, L. Miccoli, Z. Xie and J. C. Reed (1999) Lonidamine triggers apoptosis *via* a direct, Bcl-2-inhibited effect on the mitochondrial permeability transition pore. *Oncogene* **18**, 2537–2546.
58. Larochette, N., D. Decaudin, E. Jacotot, C. Brenner, I. Marzo, S. A. Susin, N. Zamzami, Z. Xie, J. Reed and G. Kroemer (1999) Arsenite induces apoptosis *via* a direct effect on the mitochondrial permeability transition pore. *Exp. Cell Res.* **249**, 413–421.
59. Miccoli, L., S. Oudard, A. Beurdeley-Thomas, B. Dutrillaux and M. F. Poupon (1999) Effect of 1-(2-chlorophenyl)-*N*-methyl-*N*-(1-methylpropyl)-3-isoquinoline carboxamide (PK11195), a specific ligand of the peripheral benzodiazepine receptor, on the lipid fluidity of mitochondria in human glioma cells. *Biochem. Pharmacol.* **58**, 715–721.
60. Woods, M. J., D. M. Zisterer and D. C. Williams (1996) Two cellular and subcellular locations for the peripheral-type benzodiazepine receptor in rat liver. *Biochem. Pharmacol.* **51**, 1283–1292.
61. Kim, H. R., Y. Luo, G. Li and D. Kessel (1999) Enhanced apoptotic response to photodynamic therapy after bcl-2 transfection. *Cancer Res.* **59**, 3429–3432.
62. Oke, B. O., C. A. Suarez-Quian, J. Riond, P. Ferrara and V. Papadopoulos (1992) Cell surface localization of the peripheral-type benzodiazepine receptor (PBR) in adrenal cortex. *Mol. Cell Endocrinol.* **87**, R1–R6.
63. Hirsch, J. D., C. F. Beyer, L. Malkowitz, C. C. Loullis and A. J. Blume (1989) Characterization of ligand binding to mitochondrial benzodiazepine receptors. *Mol. Pharmacol.* **35**, 164–172.